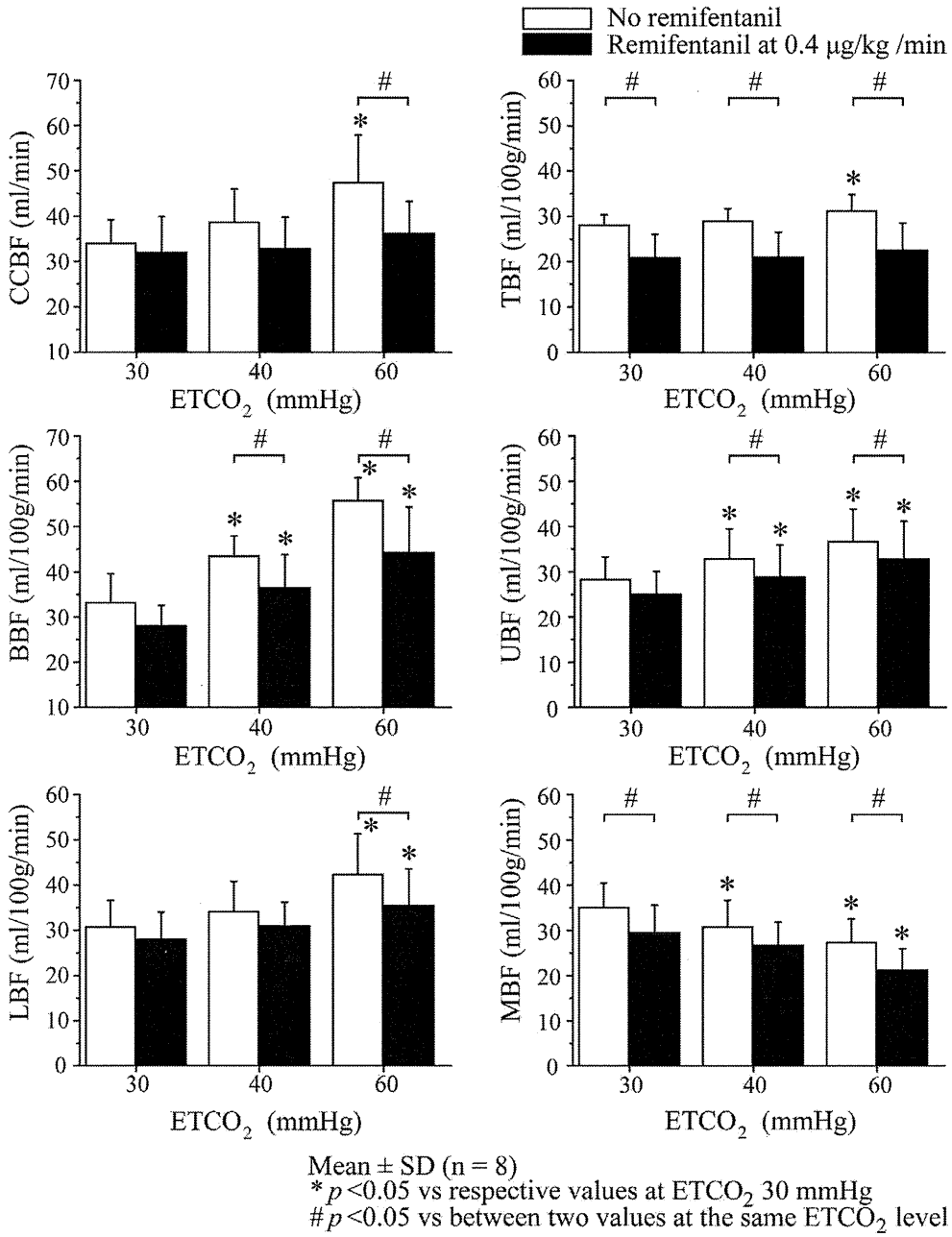

Figure 2. Comparisons of common carotid artery blood flow (CCBF), tongue mucosal blood flow (TBF), mandibular bone marrow tissue blood flow (BBF), upper alveolar tissue blood flow (UBF), lower alveolar tissue blood flow (LBF), and masseter muscle tissue blood flow (MBF) during remifentanil (Remi) infusion with those during no Remi infusion. All variables were decreased during Remi infusion when compared under identical end-tidal carbon dioxide tension ($ETCO_2$) level. The BBF, UBF, and LBF values were increased and MBF was decreased along with $ETCO_2$ elevation during Remi infusion. Data are shown as mean ± SD ($n = 8$). *$P <$ .05 versus respective values at $ETCO_2$ 30 mm Hg. #$P <$ .05 between 2 values at the same $ETCO_2$ level.

DISCUSSION

In this study, MBF was decreased and other tissue blood flows were increased at a high $ETCO_2$ level. In contrast, MBF was increased and other tissue blood flows were decreased at a low $ETCO_2$ level. When Remi was infused, all tissue blood flows were decreased. The CCBF and TBF values did not change despite $ETCO_2$ changes during Remi infusion. The CCBF, BBF, UBF, and LBF values at an $ETCO_2$ level of 60 mm Hg and MBF at an $ETCO_2$ level of 30 mm Hg during Remi infusion were comparable with those at an $ETCO_2$ level of 40 mm Hg without Remi infusion.

Handa et al[7] reported that deliberate elevation of $ETCO_2$ under isoflurane anesthesia induced increases in CCBF and BBF and a decrease in MBF, although there was no change in mandibular periosteal blood flow. In addition, HR was decreased while SBP and DBP were increased. Although the present study was performed under sevoflurane anesthesia, the results were similar to those by Handa et al.[7] Meanwhile, Koshika et al[9] reported that SBP, MAP, HR, TBF, BBF, MBF, UBF, and LBF were decreased when Remi was infused at 0.4 μg/kg/min under sevoflurane anesthesia at an $ETCO_2$ level of 35 to 40 mm Hg. In the present study, similar results were obtained at an $ETCO_2$ level of 40 mm Hg.

Hypercapnia activates the sympathetic nervous system and increases tissue blood flow.[12–14] Meanwhile, other studies have reported that skeletal muscle blood flow decreased during hypercapnia[15] or that tissue blood flow in the liver and kidneys increased while muscular blood flow decreased.[16] In the present study, similar results were observed during hypercapnia. Despite apparent hypercapnia-induced activation of the sympathetic nervous system, HR was decreased in this study. Oikawa et al[17] reported that HR was decreased in healthy rats, although renal sympathetic nervous activity was increased, during hypercapnia. When rats with parasympathetic nervous blockade were exposed to hypercapnia, an elevation of blood pressure and an activation of the sympathetic nervous system similar to those in normal rats were observed.[18] Interestingly, in these rats, the HR decrease observed in normal rats was canceled and it conversely increased. In other words, it is suggested that the decrease in HR in this study might be induced by the predominance of the parasympathetic nervous activities in the sinoatrial node. The HR further decreased when Remi was infused at a high $ETCO_2$ level. It is suggested that this result may be attributable to a negative chronotropic effect of Remi[19] in addition to the predominance of parasympathetic nervous activities in the sinoatrial node.

In this study, continuous Remi infusion depressed hypercapnia-induced increases in CCBF and TBF. James et al[20] reported that Remi decreased cardiac output. Accordingly, it is suggested that the Remi-induced decrease in cardiac output may cancel the CCBF increase during hypercapnia.

The tongue is a substantial muscle organ surrounded by a thin mucous membrane.[21] Because the thickness of the lingual mucosa in rabbits is reported to be approximately 0.5 mm[22] and the measurement depth of a laser Doppler flowmeter is approximately 0.5 mm to 1 mm,[23] it is suggested that no change in TBF may be attributable to combined measurements of tissue blood flow in both the lingual mucosa and the tongue muscle. In addition, there may be relatively greater distribution of α-receptors in the vascular smooth muscle of mucosa including the lingual mucosa.[8,24,25] Therefore, hypercapnia might produce enhanced vasoconstriction.

No change in CCBF during Remi infusion, even under hypercapnia, indicates minimal changes in total blood flow in the craniocervical area. In addition, responses of cerebral blood vessels to CO_2 is maintained during Remi infuison.[26,27] It is therefore suggested that the changes in oral tissue blood flow other than TBF under hypercapnia may result from a redistribution of muscle blood flow.

The CCBF, BBF, UBF, and LBF values at an $ETCO_2$ level of 60 mm Hg and MBF at an $ETCO_2$ level of 30 mm Hg during Remi infusion were comparable with those at an $ETCO_2$ level of 40 mm Hg without Remi infusion. These results suggest that a combination of mild hyperventilation and Remi infusion could reduce BBF without a substantial increase in MBF. This outcome could be beneficial for oral and maxillofacial surgery, including surgical invasion to the jawbone.

In this study, the infusion rate of Remi was set at 0.4 μg/kg/min based on the report of Koshika et al,[9] because this dosage clearly reduced oral tissue blood flow without a substantial decrease in blood pressure. To expose the masseter muscle and periosteum of the mandibular body, skin incisions were performed without local anesthesia to prevent lidocaine-induced changes in tissue blood flow. These surgical procedures per se might influence the tissue blood flow. However, these procedures were essential to place the needle electrodes precisely into the masseter muscle and mandibular bone marrow.

In this study, CCBF was observed as an index of total blood flow in the craniocervical region. However, because cerebral blood flow is supplied mainly by the internal carotid arteries while blood flow in the maxillofacial region is supplied by the external carotid arteries, separate observation of blood flows in the internal and external carotid arteries may allow a more detailed analysis of changes in the distribution of blood flow among tissues. Further study will be required in this respect.

In conclusion, CCBF and TBF did not change despite $ETCO_2$ changes during Remi infusion. The CCBF, BBF, UBF, and LBF values at an $ETCO_2$ level of 60 mm Hg and MBF at an $ETCO_2$ level of 30 mm Hg during Remi infusion were comparable with those at an $ETCO_2$ level of 40 mm Hg without Remi infusion.

REFERENCES

1. Fukunaga AF, Flacke WE, Bloor BC. Hypotensive effects of adenosine and adenosine triphosphate compared with sodium nitroprusside. *Anesth Analg.* 1982;61:273–278.

2. Bloor BC, Fukunaga AF, Ma C, et al. Myocardial hemodynamics during induced hypotension: a comparison

between sodium nitroprusside and adenosine triphosphate. *Anesthesiology*. 1985;63:517–525.

3. Kaneko Y. Clinical experiences and physiological response to induced hypotensive anesthesia during oral and maxillofacial surgery: especially on ATP [in Japanese]. *Shikwa Gakuho*. 1987;87:1159–1170.

4. Rodrigo C. Induced hypotension during anesthesia with special reference to orthognathic surgery. *Anesth Prog*. 1995; 42:41–58.

5. Davies DW, Greiss L, Kadar D, Steward DJ. Sodium nitroprusside in children: observations on metabolism during normal and abnormal responses. *Can Anaesth Soc J*. 1975; 22:553–560.

6. Pasch T, Huk W. Cerebral complications following induced hypotension. *Eur J Anaesthesiol*. 1986;3:299–312.

7. Handa M, Ichinohe T, Kaneko Y. Changes in partial pressure of arterial carbon dioxide induces redistribution of oral tissue blood flow in the rabbit. *J Oral Maxillofac Surg*. 2008; 66:1820–1825.

8. Kemmochi M, Ichinohe T, Kaneko Y. Remifentanil decreases mandibular bone marrow blood flow during propofol or sevoflurane anesthesia in rabbits. *J Oral Maxillofac Surg*. 2009;67:1245–1250.

9. Koshika K, Ichinohe T, Kaneko Y. Dose-dependent remifentanil decreases oral tissue blood flow during sevoflurane and propofol anesthesia in rabbits. *J Oral Maxillofac Surg*. 2011;69:2128–2134.

10. Terakawa Y, Ichinohe T, Kaneko Y. Rocuronium and vecuronium do not affect mandibular bone marrow and masseter muscular blood flow in rabbits. *J Oral Maxillofac Surg*. 2010;68:15–20.

11. Scheller MS, Saidman LJ, Partridge BL. MAC of sevoflurane in humans and the New Zealand White rabbit. *Can J Anaesth*. 1988;35:153–156.

12. Biesold D, Kurosawa M, Sato A, Trzebski A. Hypoxia and hypercapnia increase the sympathoadrenal medullary functions in anesthetized, artificially ventilated rats. *Jpn J Physiol*. 1989;39:511–522.

13. Hoka S, Arimura H, Bosnjak ZJ, Kampine JP. Regional venous outflow, blood volume, and sympathetic nerve activity during hypercapnia and hypoxic hypercapnia. *Can J Physiol Pharmacol*. 1992;70:1032–1039.

14. Dutton R, Levitzky M, Berkman R. Carbon dioxide and liver blood flow. *Bull Eur Physiopathol Respir*. 1976;12:265–272.

15. Hampson NB, Piantadosi CA, Jöbsis-vandervliet FF. Near infrared optical monitoring of cat skeletal muscle during hypercapnia. *Adv Exp Med Biol*. 1986;200:523–530.

16. Okazaki K, Okutsu Y, Fukunaga A. Effects of carbon dioxide (hypocapnia and hypercapnia) on tissue blood flow and oxygenation of liver, kidney and skeletal muscle in the dog [in Japanese]. *Masui*. 1989;38:457–464.

17. Oikawa S, Hirakawa H, Kusakabe T, Nakashima Y, Hayashida Y. Autonomic cardiovascular responses to hypercapnia in conscious rats: the roles of the chemo- and baroreceptors. *Auton Neurosci*. 2005;117:105–114.

18. Takenaka T, Hayashida Y, Kusakabe T. Cardiovascular responses in hypercapnic rats [in Japanese]. *Annu Rep Health Phys Educ Sport Sci*. 2004;23:111–112.

19. Tirel O, Chanavaz C, Bansard JY, et al. Effect of remifentanil with and without atropine on heart rate variability and RR interval in children. *Anaesthesia*. 2005;60:982–989.

20. James MK, Vuong A, Grizzle MK, Schuster SV, Shaffer JE. Hemodynamic effects of GI 87084B, an ultra-short acting mu-opioid analgesic, in anesthetized dogs. *J Pharmacol Exp Ther*. 1992;263:84–91.

21. Nakamura T. A neurohistological study on the growth of carcinoma of the tongue (VX_2 carcinoma) in domestic rabbits [in Japanese]. *J Kyushu Dent Soc*. 1991;45:76–98.

22. Iwasaki S. Morphological studies of the lingual mucosa of the rabbit-fine structure of the mucosal epithelium [in Japanese]. *Shigaku*. 1987;74:1235–1264.

23. Okamoto K, Nishikido O. Laser Doppler flowmeter [in Japanese]. *Pain Clinic*. 2008;29:1605–1612.

24. Terakawa Y, Ichinohe T, Kaneko Y. Redistribution of tissue blood flow after stellate ganglion block in the rabbit. *Reg Anesth Pain Med*. 2009;34:553–556.

25. Nishizawa S, Ichinohe T, Kaneko Y. Tissue blood flow reductions induced by remifentanil in rabbits and the effect of naloxone and phentolamine on these changes. *J Oral Maxillofac Surg*. 2012;70:797–802.

26. Klimscha W, Ullrich R, Nasel C, et al. High-dose remifentanil does not impair cerebrovascular carbon dioxide reactivity in healthy male volunteers. *Anesthesiology*. 2003; 99:834–840.

27. Ostapkovich ND, Baker KZ, Fogarty-mack P, Sisti MB, Young WL. Cerebral blood flow and CO_2 reactivity is similar during remifentanil/N_2O and fentanyl/N_2O anesthesia. *Anesthesiology*. 1998;89:358–363.

frontiers in Cellular Neuroscience

ORIGINAL RESEARCH
published: 15 June 2015
doi: 10.3389/fncel.2015.00229

Functional expression of bradykinin B_1 and B_2 receptors in neonatal rat trigeminal ganglion neurons

*Aya Kawaguchi[1], Masaki Sato[2], Maki Kimura[2], Takaki Yamazaki[3], Hitoshi Yamamoto[3], Masakazu Tazaki[2], Tatsuya Ichinohe[1] and Yoshiyuki Shibukawa[2]**

[1] Department of Dental Anesthesiology, Tokyo Dental College, Tokyo, Japan, [2] Department of Physiology, Tokyo Dental College, Tokyo, Japan, [3] Department of Histology and Developmental Biology, Tokyo Dental College, Tokyo, Japan

Bradykinin (BK) and its receptors (B_1 and B_2 receptors) play important roles in inflammatory nociception. However, the patterns of expression and physiological/pathological functions of B_1 and B_2 receptors in trigeminal ganglion (TG) neurons remain to be fully elucidated. We investigated the functional expression of BK receptors in rat TG neurons. We observed intense immunoreactivity of B_2 receptors in TG neurons, while B_1 receptors showed weak immunoreactivity. Expression of the B_2 receptor colocalized with immunoreactivities against the pan-neuronal marker, neurofilament H, substance P, isolectin B4, and tropomyosin receptor kinase A antibodies. Both in the presence and absence of extracellular Ca^{2+} ($[Ca^{2+}]_o$), BK application increased the concentration of intracellular free Ca^{2+} ($[Ca^{2+}]_i$). The amplitudes of BK-induced $[Ca^{2+}]_i$ increase in the absence of $[Ca^{2+}]_o$ were significantly smaller than those in the presence of Ca^{2+}. In the absence of $[Ca^{2+}]_o$, BK-induced $[Ca^{2+}]_i$ increases were sensitive to B_2 receptor antagonists, but not to a B_1 receptor antagonist. However, B_1 receptor agonist, Lys-[Des-Arg^9]BK, transiently increased $[Ca^{2+}]_i$ in primary cultured TG neurons, and these increases were sensitive to a B_1 receptor antagonist in the presence of $[Ca^{2+}]_o$. These results indicated that B_2 receptors were constitutively expressed and their activation induced the mobilization of $[Ca^{2+}]_i$ from intracellular stores with partial Ca^{2+} influx by BK. Although constitutive B_1 receptor expression could not be clearly observed immunohistochemically in the TG cryosection, cultured TG neurons functionally expressed B_1 receptors, suggesting that both B_1 and B_2 receptors involve pathological and physiological nociceptive functions.

Keywords: bradykinin, B_1 receptor, B_2 receptor, neuropathic pain, pain, trigeminal ganglion neuron, Ca^{2+} signaling

OPEN ACCESS

Edited by:
Pier Giorgio Mastroberardino, Erasmus University Medical Center Rotterdam, Netherlands

Reviewed by:
Emmanuel Bourinet, Institut de Génomique Fonctionnelle, France
Senthilkumar Rajagopal, Annamalai University, India

Correspondence:
Yoshiyuki Shibukawa, Department of Physiology, Tokyo Dental College, 2-9-18, Misaki-cho, Chiyoda-ku, Tokyo 101-0061, Japan
yshibuka@tdc.ac.jp

Received: *04 March 2015*
Accepted: *01 June 2015*
Published: *15 June 2015*

Citation:
Kawaguchi A, Sato M, Kimura M, Yamazaki T, Yamamoto H, Tazaki M, Ichinohe T and Shibukawa Y (2015) Functional expression of bradykinin B_1 and B_2 receptors in neonatal rat trigeminal ganglion neurons. Front. Cell. Neurosci. 9:229. doi: 10.3389/fncel.2015.00229

Introduction

Tissue damage results in an accumulation of endogenous chemical substances, such as bradykinin (BK), which are released by nociceptive afferents and/or non-neural cells in the injured area of the tissue (Julius and Basbaum, 2001; Basbaum et al., 2009). BK receptors, which are divided into two subtypes (B_1 and B_2), are plasma membrane G-protein-coupled receptors of the seven-transmembrane-domain family. The existence of B_1 and B_2 receptors has been confirmed by pharmacological and radioligand-binding studies, as well as by mRNA expression analyses, in a wide variety of cells (Hess et al., 1994; Pesquero et al., 1996; Hall, 1997).

Previous studies have indicated that B_2 receptors couple with the Gq protein. Activation of the Gq protein activates phospholipase C, which induces a number of intracellular second messenger systems, including 1, 2-diacylglycerol and inositol 1, 4, 5-trisphosphate, which activates protein kinase C and mobilizes intracellular Ca^{2+}, respectively (Walker et al., 1995; Tiwari et al., 2005).

BK-induced changes in the chemical environment surrounding axons cause peripheral sensitization, which is associated with inflammatory responses (Basbaum et al., 2009). Neuropathic pain is also involved in peripheral and central sensitization, which increases chronic pain states (Cervero and Laird, 1996; Scholz and Woolf, 2002; Ochoa, 2009). Injury to trigeminal ganglion (TG) neurons, which occasionally induces neuropathic pain, has been reported to be mediated by both B_1 and B_2 receptors in the orofacial area. Formalin-induced orofacial pain responses in rats are reduced by B_2 receptor inhibition (Chichorro et al., 2004). In addition, administration of B_1 and B_2 receptor antagonists delays the development of thermal hyperalgesia in the orofacial area, which is induced by constriction of the infraorbital nerve in rats and mice (Luiz et al., 2010). Thus, the functional role of BK receptors in TG neurons in physiological and pathological nociception has been well described by behavioral studies. However, the basic expression patterns of B_1 and B_2 receptors in TG neurons are still unclear and remain to be fully elucidated.

In the present study, we investigated the expression and localization, as well as physiological and pharmacological properties, of B_1 and B_2 receptors in primary cultured rat TG neurons.

Materials and Methods

Ethical Approval

All the animals used in our study were treated in accordance with the Guiding Principles for the Care and Use of Animals in the Field of Physiological Sciences, which was approved by the Council of the Physiological Society of Japan and the American Physiological Society. In addition, the study followed the guidelines that were established by the National Institutes of Health (USA) regarding the care and use of animals for experimental procedures. This study was approved by the Animal Research Ethics Committee of Tokyo Dental College (approval No. 252502).

Cell Culture

TG cells were isolated from neonatal Wistar rats (7 days old) (Kawaguchi et al., 2015) that were under pentobarbital sodium anesthesia (50 mg/kg) following the administration of isoflurane (3.0 Vol%). TG cells were dissociated by enzymatic treatment with Hank's balanced salt solution (Life Technologies, Grand Island, NY, USA) containing 20 U/mL papain (Worthington Biochemical Corporation, Lakewood, NJ, USA) for 20 min at 37°C, which was followed by dissociation by trituration. After dissociation, the TG cells were plated on 35 mm-diameter dishes (Corning Incorporated Life Sciences, Tewksbury, MA, USA) and cultured for 48 h at 37°C (95% air and 5% CO_2). The primary cells were cultured in Leibovitz's L-15 medium (Life Technologies) containing 10% fetal bovine serum, 1% penicillin-streptomycin (Life Technologies), 1% fungizone (Life Technologies), 26 mM $NaHCO_3$, and 30 mM glucose (pH 7.4). For the immunocytochemistry, TG cells were subjected to primary culture on poly-L-lysine-coated cover glasses (Matsunami Glass Ind., Ltd., Osaka, Japan).

Immunofluorescence Analysis

TGs isolated from neonatal Wistar rats (7 days old) were fixed in optimal cutting temperature compound and rapidly frozen in liquid nitrogen. Frozen tissues were cut at a thickness of 10 μm and placed on slides. After fixation by 50% ethanol and 50% acetone at −20°C for 30 min, primary cultured TG cells and cryosections were treated with 10% donkey serum at room temperature for 20 min and then incubated overnight at 4°C with primary antibodies (Kuroda et al., 2013). A cocktail of primary antibodies (Neuro-Chrom^{TM} Pan Neuronal Marker, EMD Millipore, Billerica, MA, USA; 1:50 dilution), including mouse anti-Neuronal nuclei (NeuN), anti-microtubule-associated protein 2 (MAP2), anti-βIII tubulin, and anti-neurofilament H (NF-H) antibodies, was used as a neuronal marker. TG cells were also incubated with either mouse anti-NF-H (SantaCruz, CA, USA; 1:200 dilution) as an A-neuron marker, mouse anti-substance P (SP; R&D Systems, Minneapolis, MN, USA; 2.5 μg/100 μl dilution) as a peptidergic C-neuron marker, FITC-conjugated anti-isolectin B4 (IB4; Vector laboratories, CA, USA; 1:200 dilution) as a non-peptidergic C-neuron marker, goat anti-high-affinity nerve growth factor (NGF) receptor (a tropomyosin receptor kinase A (TrkA); R&D Systems; 1.5 μg/100 μl dilution) as an NGF-responsive nociceptor marker (Mantyh et al., 2011), and rabbit anti-B_1 receptor (Alomone Labs, Jerusalem, Israel; 1:50 dilution) and rabbit anti-B_2 receptor (Alomone Labs; 1:50 dilution) (Duehrkop et al., 2013; Dutra et al., 2013) antibodies. For negative controls, the sections were incubated with non-immune IgGs (Abcam, Cambridge, UK; 1:50; N = 4 from four rats) (**Figure 2M**). The cells and tissues were then washed and incubated with a secondary antibody at room temperature for 30 min. The secondary antibodies were Alexa Fluor 488 donkey anti-rabbit IgG, Alexa Fluor 568 donkey anti-mouse IgG, Alexa Fluor 568 donkey anti-rabbit IgG, and Alexa Fluor 568 donkey anti-goat IgG (1:50 dilution; Life Technologies) for the fluorescence staining and 4′, 6-diamino 2-phenylindole dihydrochloride (Life Technologies) for the nuclear staining (room temperature for 5 min). The cells and tissues were examined under fluorescence microscopes (Carl Zeiss AG, Jena, Germany; Keyence Corporation, Osaka, Japan).

Solutions and Reagents

A standard solution containing (in mM) 137 NaCl, 5.0 KCl, 2.0 $CaCl_2$, 0.5 $MgCl_2$, 0.44 KH_2PO_4, 0.34 Na_2HPO_4, 4.17 $NaHCO_3$, and 5.55 glucose (pH 7.4) was used as an extracellular solution. A high-K^+ solution containing (in mM) 91 NaCl, 50 KCl, 2.0 $CaCl_2$, 0.5 $MgCl_2$, 0.44 KH_2PO_4, 0.34 Na_2HPO_4, 4.17 $NaHCO_3$, and 5.55 glucose (pH 7.4) was used to discern TG neurons from

glial cells by activation of depolarization-induced increases in intracellular free Ca^{2+} concentration ($[Ca^{2+}]_i$) in neurons. BK, a selective B_2 receptor antagonist (HOE140), a selective B_1 receptor antagonist (R715) and a highly selective B_1 receptor agonist (Lys-[Des-Arg^9]BK) were obtained from Tocris Bioscience (Bristol, UK). All the other reagents were purchased from Sigma-Aldrich Co. LLC (St. Louis, MO, USA), except where indicated.

Measurement of $[Ca^{2+}]_i$

Primary cultured TG cells were loaded for 90 min at 37°C in Hank's solution containing 10 μM of fura-2 acetoxymethyl ester (Dojindo Laboratories, Kumamoto Japan) and 0.1% (w/v) pluronic acid F-127 (Life Technologies). Cultured TG cells were then rinsed with fresh Hank's solution and mounted on a microscope stage (Olympus Corporation, Tokyo, Japan). Fura-2 fluorescence emission was measured at 510 nm in response to alternating excitation wavelengths of 340 nm ($F340$) and 380 nm ($F380$) with an Aquacosmos system and software (Hamamatsu Photonics K.K., Shizuoka, Japan), which controls the excitation wavelength selector and intensified charge-coupled device camera system (Hamamatsu Photonics K.K.). $[Ca^{2+}]_i$ was measured as the fluorescence ratio of $F340$ and $F380$ ($R_{F340/F380}$) and expressed as F/F_0 units. The $R_{F340/F380}$ value (F) was normalized to the resting value (F_0).

Statistical and Offline Analysis

The data were expressed as the mean ± standard error (S.E.) or standard deviation of the mean of N observations, where N represents the number of independent experiments or cells, respectively. The Kruskal–Wallis test, Dunn's posthoc test, or Mann–Whitney U-test was used to determine the nonparametric statistical significance. P values less than 0.05 were considered significant. The statistical analysis was performed with GraphPad Prism 5.0 (GraphPad Software, Inc., La Jolla, CA, USA).

The dependence of the changes in $[Ca^{2+}]_i$ on each pharmacological agent was determined by fitting the data to the following function with Origin 8.5 (OriginLab Corporation, Northampton, MA, USA):

$$F/F_0 = \left[(F/F_{0\text{int}} - F/F_{0\text{fin}})/(1 + ([x]_o/K))\right] + F/F_{0\text{fin}} \quad (1)$$

where K is the equilibrium binding constant, $[x]_o$ indicates the applied concentration of the pharmacological agents, and $F/F_{0\text{int}}$ and $F/F_{0\text{fin}}$ are the initial and final F/F_0 responses, respectively.

Results

Immunolocalization of BK Receptors in TG Neurons

The cultured TG neurons showed positive immunoreactivity to a neuronal marker cocktail (Neuro-Chrom^{TM} pan-neuronal marker), which contained mouse anti-NeuN, anti-MAP2, and anti-βIII tubulin antibodies (**Figures 1A,D**). Intense B_2 receptor immunoreactivity was observed in primary cultured TG neurons (**Figure 1E**), and it showed colocalization with the pan neuronal marker (**Figure 1F**) in somata, dendrites, axons, and perinuclear regions. Weak but positive B_1 receptor immunoreactivity was also observed in primary cultured TG cells (**Figure 1B**), and the immunoreactivity colocalized with the pan neuronal marker (**Figure 1C**).

In the TG cryosections, we could observe positive immunoreactivity against the neuronal marker cocktail (**Figures 1G,J**). These TG neurons in the cryosections showed positive immunoreactivity to the B_2 receptor antibody (**Figure 1K**), showing colocalization with the pan neuronal marker (**Figure 1L**) in somata, dendrites, axons, and perinuclear regions. However, the TG cryosections did not show B_1 receptor immunoreactivity (**Figures 1H,I**). Positive immunoreactivity was also observed with NF-H (an A-neuron marker; **Figure 2A**), SP (a peptidergic C-neuron marker; **Figure 2D**), IB4 (a non-peptidergic C-neuron marker; **Figure 2G**), and high-affinity NGF receptor (TrkA; an NGF-responsive nociceptor marker; **Figure 2J**) antibodies. These immunoreactivities against NF-H, SP, IB4, and TrkA antibodies showed colocalization with those against the B_2 receptor antibodies (**Figures 2B,C,E,F,H,I,K,L**).

BK-Induced $[Ca^{2+}]_i$ Increases in TG Neurons

We observed rapid and transient $[Ca^{2+}]_i$ increases in TG neurons following the administration of five different concentrations of BK (0.01, 0.1, 1.0, 10, and 100 nM) in the presence of external Ca^{2+} (2.0 mM; **Figure 3A**). A semilogarithmic plot (**Figure 3B**) illustrates F/F_0 values as a function of the applied BK concentrations, and the equilibrium-binding constant was the half-maximal 50% effective concentration (EC_{50}) of 1.0 nM.

HOE140, a B_2 Receptor Antagonist, Inhibited the BK-Induced $[Ca^{2+}]_i$ Increases in TG Neurons

We examined the BK-induced $[Ca^{2+}]_i$ responses in both the presence and absence of external Ca^{2+}. The application of BK (1.0 nM) rapidly increased $[Ca^{2+}]_i$ to a peak F/F_0 value of 1.7 ± 0.03 F/F_0 units in the presence (2.0 mM) of external Ca^{2+} and 1.4 ± 0.03 F/F_0 units in the absence (0 mM) of external Ca^{2+} (**Figures 4A,D**). The amplitudes of the BK-induced $[Ca^{2+}]_i$ increases significantly differed between those in the presence and absence of extracellular Ca^{2+}. In the absence of extracellular Ca^{2+}, BK (1.0 nM)-induced $[Ca^{2+}]_i$ increases were significantly inhibited by a B_2 receptor antagonist (100 nM of HOE140) (**Figures 4C,D**) but not by a B_1 receptor antagonist (1.0 μM of R715) (**Figures 4B,D**).

The B_1 Receptor Antagonist R715 did not Affect the BK-Induced $[Ca^{2+}]_i$ Increases

The BK-induced (1.0 nM) increases in $[Ca^{2+}]_i$ were not significantly inhibited in TG neurons by the administration of four different concentrations of the B_1 receptor antagonist (0.001, 0.01, 0.1, and 1.0 μM of R715) in the presence (2.0 mM) of external Ca^{2+} (**Figures 5A,B**).

Pharmacological Identification of B_1 Receptors in TG Neurons

We investigated the $[Ca^{2+}]_i$ increases during the administration of Lys-[Des-Arg^9]BK, which is an endogenous, potent, and

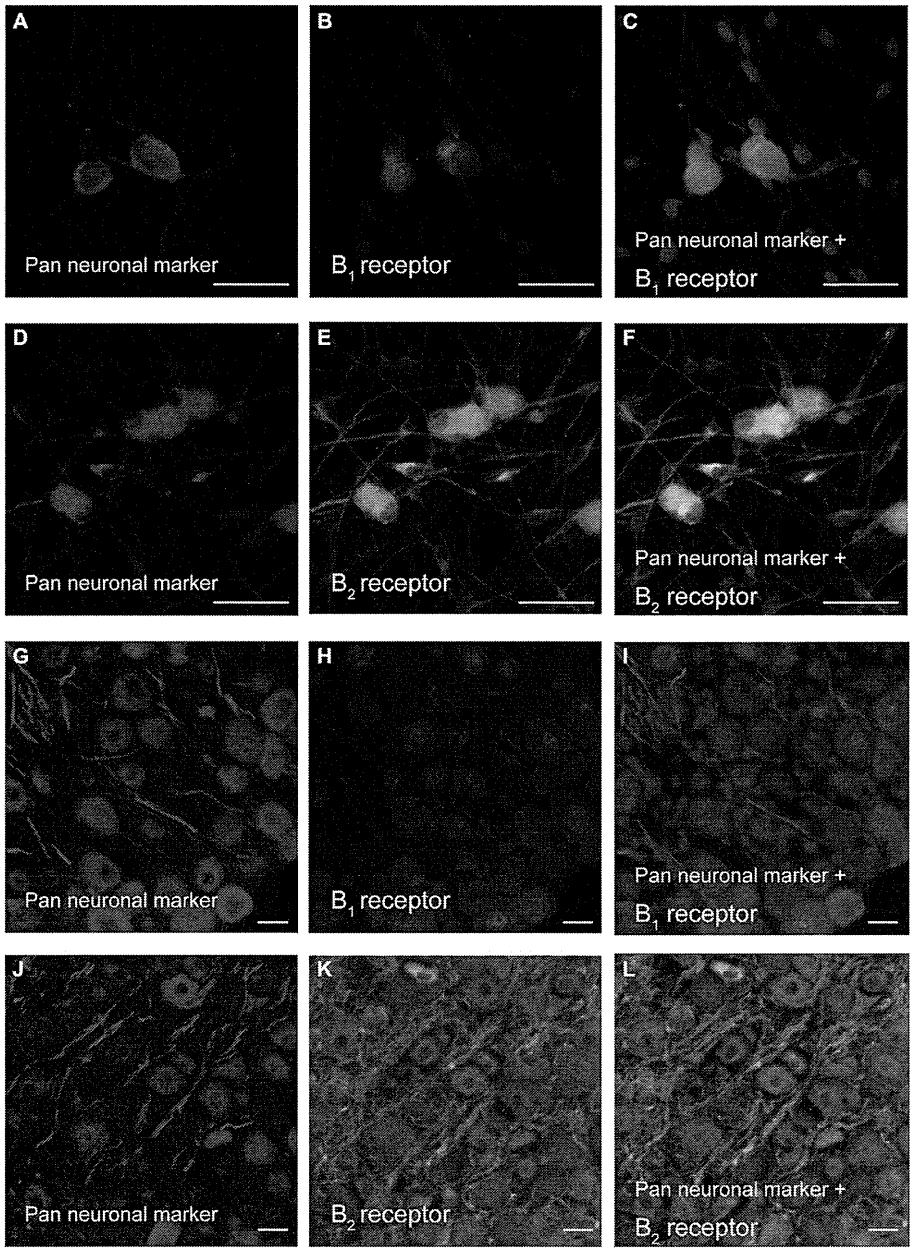

FIGURE 1 | Immunolocalization of B_1 and B_2 receptors in primary cultured trigeminal ganglion (TG) neurons and TG cryosections. **(A,D,G,J)** Cells positive for the pan neuronal marker in primary cultured TG neurons **(A,D)** and TG cryosections **(G,J)**. **(B,H)** Immunoreactivity to the B_1 receptor antibody (green) in primary cultured TG neurons **(B)** and TG cryosections **(H)**. **(C,I)** Triple immunofluorescence staining with antibodies against the pan neuronal marker (red) and B_1 receptor (green) in primary cultured TG neurons **(C)** and TG cryosections **(I)**. Nuclei are shown in blue. **(E,K)** Positive immunoreactivity to the B_2 receptor antibody (green) in primary cultured TG neurons **(E)** and TG cryosections **(K)**. **(F,L)** Triple immunofluorescence staining with antibodies against the pan neuronal marker (red) and B_2 receptor (green) in primary cultured TG neurons **(F)** and TG cryosections **(L)**. Nuclei are shown in blue. Scale bars are 50 μm in **(A–F)**, and 20 μm in **(G–L)**. Each set of images showing representative immunolocalization of B_1 **(A–C)** and B_2 receptors **(D–F)** in primary cultured TG neurons was obtained from six different rats, while that showing immunolocalization of B_1 **(G–I)** and B_2 receptors **(J–L)** in TG cryosections was obtained from five different rats.

highly selective B_1 receptor agonist (Talbot et al., 2009; More et al., 2014). The increases in $[Ca^{2+}]_i$ in the TG neurons were induced by the administration of five different concentrations of Lys-[Des-Arg^9]BK (0.01, 0.1, 1, 10, and 100 nM) in the presence of extracellular Ca^{2+} (2.0 mM) (**Figure 5C**). A semilogarithmic plot (**Figure 5D**) illustrates the F/F_0 values as a function of the applied concentration of Lys-[Des-Arg^9]BK with an equilibrium-binding constant of 0.4 nM. In the presence of extracellular

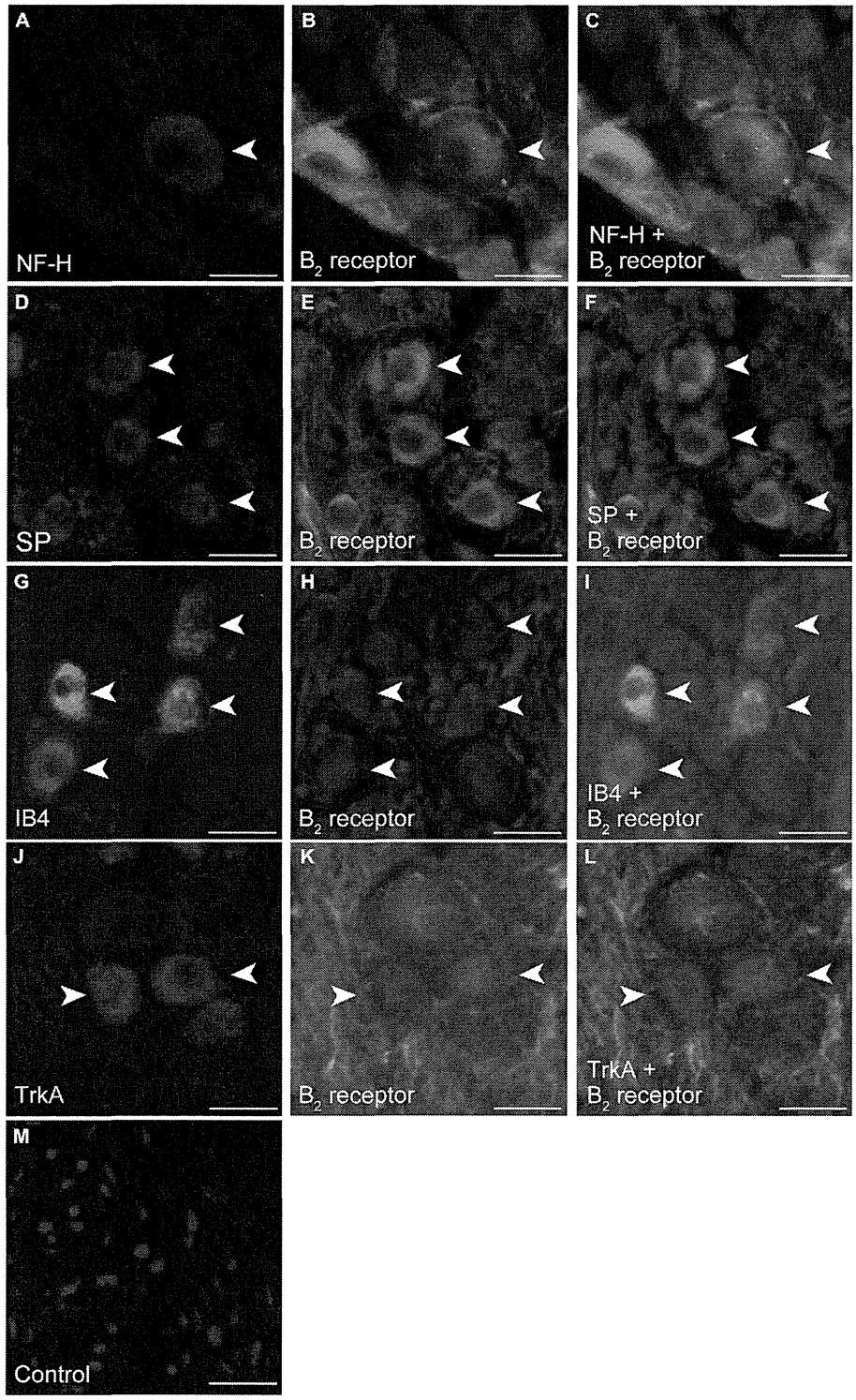

FIGURE 2 | Immunolocalization of B_2 receptors in the soma of TG neurons in cryosections. (A) Positive immunoreactivity to NF-H as an A-neuron marker in TG neurons (arrowhead). **(B,E,H,K)** B_2 receptor immunoreactivity (arrowheads). **(C)** Triple immunofluorescence staining with antibodies against B_2 receptors (green) and NF-H (red). Nuclei are shown in blue. **(D)** Positive immunoreactivity to SP as a peptidergic C-neuron marker in TG neurons (arrowheads). **(F)** Triple staining with antibodies against B_2 receptors (green) and SP (red). Nuclei are shown in blue. **(G)** Positive immunoreactivity to IB4 as a non-peptidergic C-neuron marker in TG neurons (arrowheads). **(I)** Triple staining with antibodies against B_2 receptors (red) and IB4 (green). Nuclei are shown in blue. **(J)** Positive immunoreactivity to TrkA as an nerve growth factor (NGF)-responsive nociceptor marker in TG neurons (arrowheads). **(L)** Triple staining with antibodies against B_2 receptors (green)

(*Continued*)

FIGURE 2 | Continued
and TrkA (red). Nuclei are shown in blue. **(M)** No fluorescence was detected in the negative control. Scale bars: 20 μm. Each set of photos showing representative colocalization of B_2 receptors with NF-H **(A–C)** and SP **(D–F)** was obtained from six different rats. Each set of photos showing representative colocalization of B_2 receptors with IB4 **(G–I)** and TrkA **(J–L)** was obtained from four different rats.

Ca^{2+}, the Lys-[Des-Arg^9]BK-induced increase in $[Ca^{2+}]_i$ was significantly inhibited by a B_1 receptor antagonist (1.0 μM of R715) (**Figures 5E,F**).

Discussion

The present study demonstrated the functional expression of BK receptors (B_1 and B_2) in TG neurons. B_2 receptors were present on axons and dendrites in A-neurons, non-peptidergic C-neurons, peptidergic C-neurons, and NGF-responsive nociceptors. While the localization pattern of the B_1 receptor was not clear in the TG cryosections, weak immunoreactivity for B_1 receptors was observed in the primary cultured TG neurons. The application of BK activated B_2 receptors and Lys-[Des-Arg^9]BK activated the B_1 receptors. B_2 receptor activation mobilized $[Ca^{2+}]_i$ by releasing Ca^{2+} from internal Ca^{2+} stores with partial Ca^{2+} influx from the extracellular medium.

B_2 receptors, which are expressed ubiquitously and constitutively in healthy tissues, are essential in the early stages of general pain generation (Hall, 1992). The constitutive expression of B_2 receptors in TG neurons has been studied by reverse transcription-polymerase chain reaction (RT-PCR) analyses (Ceruti et al., 2011) and immunocytochemical analyses in cultured TG neurons (Patwardhan et al., 2005). Although BK-induced $[Ca^{2+}]_i$ increases have also been reported in TG neurons (Ceruti et al., 2008, 2011), precise functional expression patterns of B_1 and B_2 receptors in TG neurons remained unclear. The results of the present study showing the functional expression and localization of B_2 receptors in TG neurons were in line with the previous results. The results of this study were also in line with the pharmacological properties of BK, which is a potent and endogenous agonist for B_2 receptors and not B_1 receptors in the sympathetic neurons of the rat superior cervical ganglion (Babbedge et al., 1995) and in Chinese hamster ovary (CHO) cells stably expressing recombinant human B_1 or B_2 receptors (Simpson et al., 2000). Furthermore, BK has an affinity for B_2 receptors that is 500 times that for B_1 receptors (Simpson et al., 2000). Therefore, B_2 receptors are histologically and functionally expressed, and endogenous BK preferentially activates B_2 receptors in rat TG neurons.

The expression of the B_1 receptor, which is induced as a result of tissue damage and inflammation, is involved in chronic inflammation or tissue injury (Hall, 1992). The observations of the constitutive B_1 receptor expression in TG and dorsal root ganglion (DRG) neurons have been inconsistent. In DRG neurons, some immunohistochemical studies have reported constitutive B_1 receptor expression (Ma et al., 2000; Wotherspoon and Winter, 2000). In contrast, other studies have described that B_1 receptor activation-induced $[Ca^{2+}]_i$ responses could not be observed in DRG neurons (Brand et al., 2001). In TG neurons, an immunohistochemical study has shown the constitutive expression of B_1 receptors (Ma et al., 2000). In contrast, RT-PCR analyses have demonstrated that B_1 receptor mRNA was barely expressed in intact tissue, while it was weakly

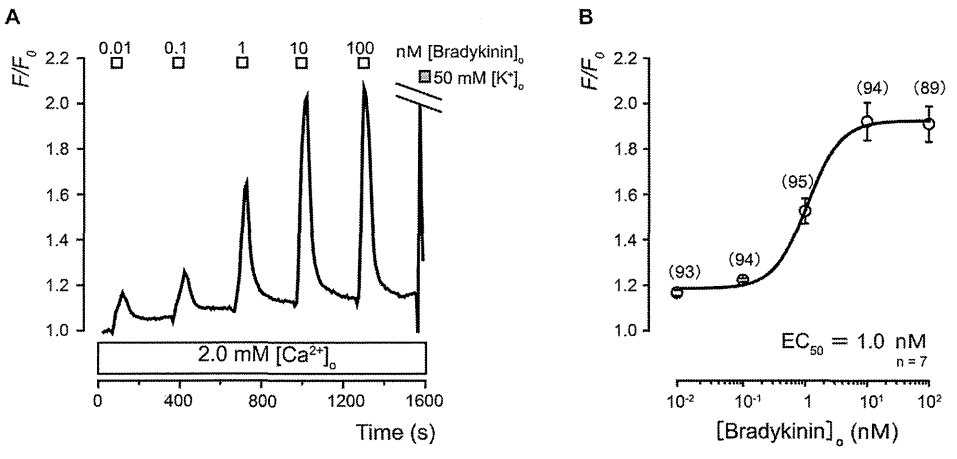

FIGURE 3 | Ca^{2+} dependence of extracellular bradykinin (BK)-induced $[Ca^{2+}]_i$ responses in TG neurons. **(A)** Examples of transient $[Ca^{2+}]_i$ increases following the application of a series of BK concentrations. In the presence of extracellular Ca^{2+} (2.0 mM; lower white box), the application of BK induced transient $[Ca^{2+}]_i$ increases in a concentration-dependent manner. The concentrations of BK (0.01–100 nM) that were administered are shown in the uppermost white boxes. **(B)** The data points illustrate the F/F_0 values as a function of the applied BK concentration. Each data point represents the mean ± standard error (S.E.) of seven experiments (the numbers in parentheses represent the number of tested cells). The curve on the semilogarithmic scale was fitted according to *Equation 1*, which is described in the text. The upper gray box in **(A)** indicates the timing of the application of the 50 mM KCl solution. The equilibrium binding constant of BK was 1.0 nM.

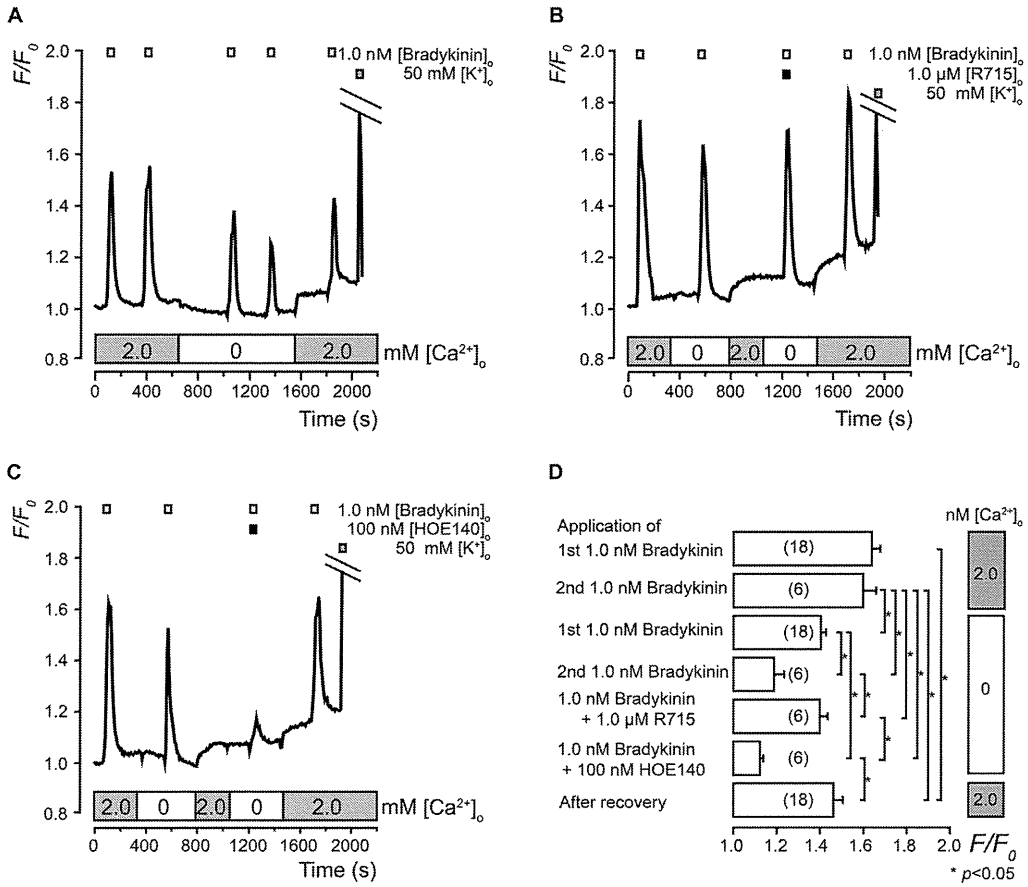

FIGURE 4 | Pharmacological identification of BK receptors in TG neurons. **(A)** Examples of transient $[Ca^{2+}]_i$ increases following the administration of 1.0 nM of BK (upper white boxes) with (lower gray boxes) or without (lower white box) extracellular Ca^{2+} (2.0 mM). **(B)** Examples of BK-induced (1.0 nM; upper white boxes) $[Ca^{2+}]_i$ increases with (upper black box) or without R715 in the absence (lower white box) or presence (lower gray boxes) of external Ca^{2+}. **(C)** Examples of BK-induced (1.0 nM; upper white boxes) $[Ca^{2+}]_i$ increases with (upper black box) or without HOE140 in the absence (lower white box) or presence (lower gray boxes) of external Ca^{2+}. **(A,B,C)** The upper gray boxes indicate the timing of the application of the 50 mM of KCl solution. **(D)** The summary bar graph indicates $[Ca^{2+}]_i$ increases during the first (upper column) and second (second upper column) application of 1.0 nM of BK with external Ca^{2+} (2.0 mM) (gray boxes on the right side). The mean values of the increase in $[Ca^{2+}]_i$ following the first (third upper column) and second (fourth upper column) application of 1.0 nM of BK in the absence of external Ca^{2+} as well as the application of 1.0 nM of BK with 1.0 μM of R715 (fifth upper column) and 100 nM of HOE140 (sixth upper column) in the absence of external Ca^{2+} (white boxes on the right side) are shown. Each column denotes the mean ± S.E. of the indicated (in parentheses) number of experiments. The statistical significance between the columns (shown by solid lines) is indicated by asterisks: $*p < 0.05$.

expressed in primary cultured TG neurons. In primary cultured TG neurons, the levels of expression of B_1 receptor mRNA have been reported to depend on the length of the culture period (Ceruti et al., 2011). The present immunohistochemical and immunocytochemical results were similar to the previous RT-PCR results; B_1 receptor immunoreactivity was weakly positive in cultured TG neurons and could not be detected in intact TG tissue. Although few report concerning B_1 receptor-induced $[Ca^{2+}]_i$ response in TG neurons exist, in the $[Ca^{2+}]_i$ imaging in the present study, the B_1 receptor agonist, Lys-[Des-Arg^9]BK which is a metabolite of endogenous BK in peripheral tissues (Regoli et al., 2001), dose-dependently increased $[Ca^{2+}]_i$ in the presence of extracellular Ca^{2+}, and this increase was suppressed by a B_1 receptor-specific antagonist (**Figures 5C–F**). These results of B_1 receptor expression in primary cultured TG neurons suggest that the expression of B_1 receptors is induced in TG neurons by tissue damage and/or inflammation. However, further studies are required to evaluate the expression patterns of B_1 receptors in native TG neurons.

BK-induced $[Ca^{2+}]_i$ increases were observed in both the presence and absence of extracellular Ca^{2+}. However, the amplitudes of the $[Ca^{2+}]_i$ increases in the absence of extracellular Ca^{2+} were significantly smaller (84.9 ± 11.3%, N = 161) than those in the presence of Ca^{2+} (100%; **Figures 4A,D**). This indicated that the BK-induced $[Ca^{2+}]_i$ mobilization (by B_2 receptor activation) was mainly composed of Ca^{2+} release from internal stores with partial Ca^{2+} influx from the extracellular medium. Notably, BK has been reported to activate voltage-dependent Ca^{2+} channels in rat submucosal

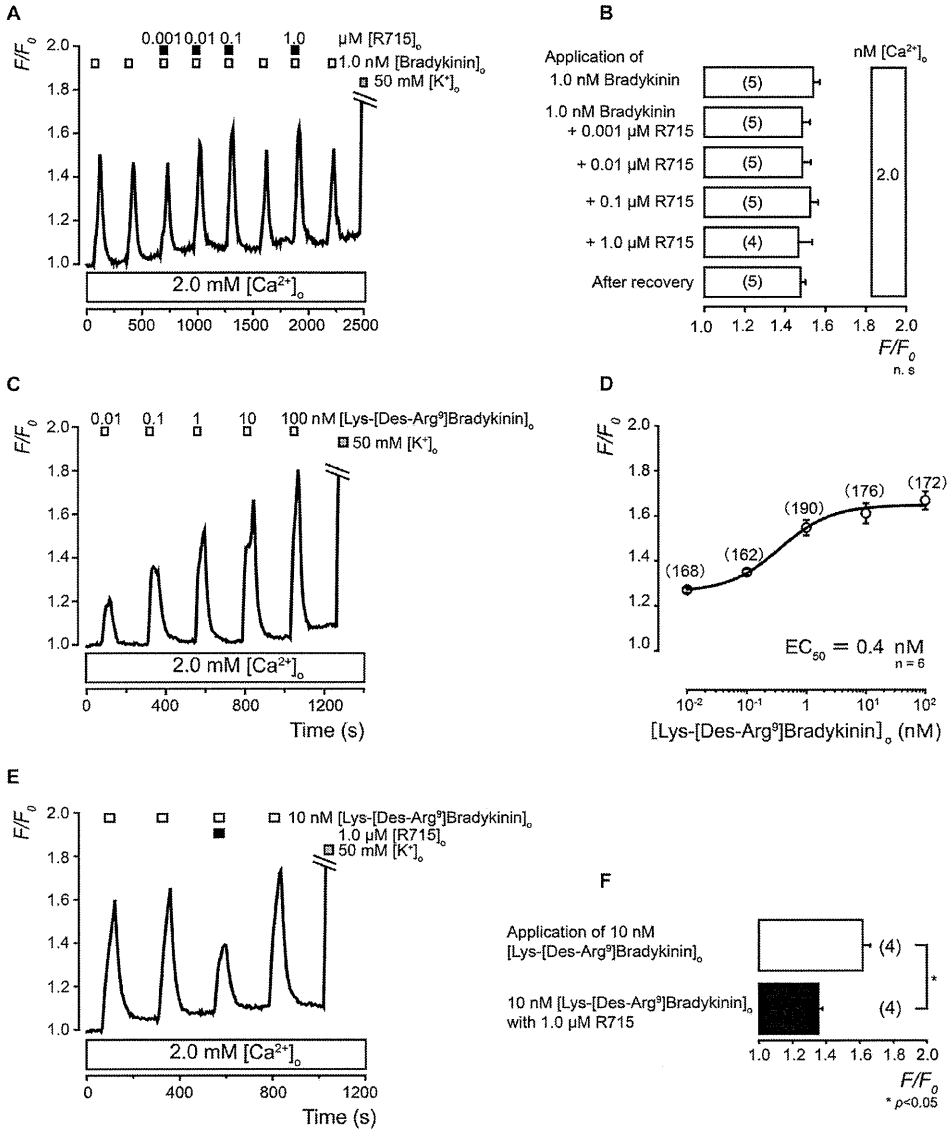

FIGURE 5 | Pharmacological identification of B_1 receptors in TG neurons. **(A)** Examples of BK-induced (1.0 nM; upper white boxes) $[Ca^{2+}]_i$ increases showing insensitivity to R715 (0.001–1.0 μM; upper black boxes) in the presence of external Ca^{2+} (2.0 mM; lower white box). **(B)** The summary bar graph indicates $[Ca^{2+}]_i$ increases following the first (upper column) application of 1.0 nM of BK with external Ca^{2+} (2.0 mM). The mean values for the increases in $[Ca^{2+}]_i$ following the application of 1.0 nM of BK with 0.001 μM (second upper column), 0.01 μM (third upper column), 0.1 μM (fourth upper column), or 1.0 μM (fifth upper column) of R715 in the presence of external Ca^{2+} (white boxes on the right side) are shown. Each column denotes the mean ± S.E. of the indicated (in parentheses) number of experiments. There is no statistical significance between the columns. **(C)** Examples of transient $[Ca^{2+}]_i$ increases following the application of a series of concentrations of Lys-[Des-Arg^9]BK (0.01–100 nM; upper white boxes) in the presence of extracellular Ca^{2+} (2.0 mM; lower white box). **(D)** The data points illustrate the F/F_0 values as a function of the applied concentrations of Lys-[Des-Arg^9]BK. Each data point represents the mean ± S.E. of six independent experiments (the numbers in parentheses represent the number of tested cells). The curve on the semilogarithmic scale was fitted according to *Equation 1*, which is described in the text. The equilibrium-binding constant for Lys-[Des-Arg^9]BK was 0.4 nM. **(E)** Examples of Lys-[Des-Arg^9]BK-induced (10 nM; upper white boxes) $[Ca^{2+}]_i$ increases that were significantly inhibited by 1.0 μM of R715 (upper black box) in the presence of external Ca^{2+} (2.0 mM; lower white box). **(A,C,E)** The application of 50 mM of the KCl solution is shown in the gray boxes. **(F)** Summary bar graph of the $[Ca^{2+}]_i$ increases following 10 nM of Lys-[Des-Arg^9]BK with (lower black column) or without (upper white column) 1.0 μM of R715. Each column denotes the mean ± S.E. of the indicated number (in parentheses) of independent experiments. The statistical significance between the columns (shown by solid lines) is indicated by asterisks: *p < 0.05.

plexus neurons (Avemary and Diener, 2010; Rehn et al., 2013), and transient receptor potential cation channel subfamily-V member-1 channels in rat DRG neurons (Ferreira et al., 2004; Mistry et al., 2014). However, BK-induced Ca^{2+} currents could not be recorded in TG neurons (Kitakoga and Kuba, 1993). Although further studies are needed to clarify which Ca^{2+}

influx pathways contribute to the BK-induced Ca^{2+} influx in TG neurons, the present results clearly indicate that BK mobilizes $[Ca^{2+}]_i$ through both intracellular Ca^{2+} release and Ca^{2+} influx.

In addition, NGF-TrkA signaling plays important roles in not only the developmental processes of peptidergic nociceptive afferents, but also in the generation of acute and chronic pain state in adults. The signaling also up-regulates B_2 receptor expression in peptidergic nociceptors (Mantyh et al., 2011). Thus, the results showing colocalization of B_2 receptor and TrkA immunoreactivity in TG neurons strongly support reports describing that the B_2 receptor mediates inflammatory/neuropathic pain induced by peripheral sensitization in the orofacial region (Chichorro et al., 2004; Luiz et al., 2010); however, the present results obtained from neonatal rat may not reflect the situation in adults.

In conclusion, B_2 receptors were expressed constitutively, and their activation induced the mobilization of $[Ca^{2+}]_i$ by releasing Ca^{2+} from intracellular stores with partial Ca^{2+} influx. In contrast, B_1 receptor expression was faint in cultured TG neurons and absent in neurons in TG cryosections, although a metabolite of endogenous BK elicited $[Ca^{2+}]_i$ increases. These results indicated that both BK and its metabolites activated $[Ca^{2+}]_i$ mobilization in TG neurons through B_2 and B_1 receptor activation, respectively.

Acknowledgments

This research was supported by a Grant-in-Aid (#23592751/26861559/25861762) for Scientific Research from the Ministry of Education, Culture, Sports, Science, and Technology of Japan.

References

Avemary, J., and Diener, M. (2010). Bradykinin-induced depolarisation and Ca^{2+} influx through voltage-gated Ca^{2+} channels in rat submucosal neurons. *Eur. J. Pharmacol.* 635, 87–95. doi: 10.1016/j.ejphar.2010.03.009

Babbedge, R., Dray, A., and Urban, L. (1995). Bradykinin depolarises the rat isolated superior cervical ganglion via B_2 receptor activation. *Neurosci. Lett.* 193, 161–164. doi: 10.1016/0304-3940(95)11690-x

Basbaum, A. I., Bautista, D. M., Scherrer, G., and Julius, D. (2009). Cellular and molecular mechanisms of pain. *Cell* 139, 267–284. doi: 10.1016/j.cell.2009.09.028

Brand, M., Klusch, A., Kurzai, O., Valdeolmillos, M., Schmidt, R. F., and Petersen, M. (2001). No evidence for bradykinin B_1 receptors in rat dorsal root ganglion neurons. *Neuroreport* 12, 3165–3168. doi: 10.1097/00001756-200110080-00036

Ceruti, S., Fumagalli, M., Villa, G., Verderio, C., and Abbracchio, M. P. (2008). Purinoceptor-mediated calcium signaling in primary neuron-glia trigeminal cultures. *Cell Calcium* 43, 576–590. doi: 10.1016/j.ceca.2007.10.003

Ceruti, S., Villa, G., Fumagalli, M., Colombo, L., Magni, G., Zanardelli, M., et al. (2011). Calcitonin gene-related peptide-mediated enhancement of purinergic neuron/glia communication by the algogenic factor bradykinin in mouse trigeminal ganglia from wild-type and R192Q Cav2.1 Knock-in mice: implications for basic mechanisms of migraine pain. *J. Neurosci.* 31, 3638–3649. doi: 10.1523/JNEUROSCI.6440-10.2011

Cervero, F., and Laird, J. M. (1996). Mechanisms of touch-evoked pain (allodynia): a new model. *Pain* 68, 13–23. doi: 10.1016/s0304-3959(96)03165-x

Chichorro, J. G., Lorenzetti, B. B., and Zampronio, A. R. (2004). Involvement of bradykinin, cytokines, sympathetic amines and prostaglandins in formalin-induced orofacial nociception in rats. *Br. J. Pharmacol.* 141, 1175–1184. doi: 10.1038/sj.bjp.0705724

Duehrkop, C., Banz, Y., Spirig, R., Miescher, S., Nolte, M. W., Spycher, M., et al. (2013). C1 esterase inhibitor reduces lower extremity ischemia/reperfusion injury and associated lung damage. *PLoS One* 8:e72059. doi: 10.1371/journal.pone.0072059

Dutra, R. C., Bento, A. F., Leite, D. F. P., Manjavachi, M. N., Marcon, R., Bicca, M. A., et al. (2013). The role of kinin B_1 and B_2 receptors in the persistent pain induced by experimental autoimmune encephalomyelitis (EAE) in mice: evidence for the involvement of astrocytes. *Neurobiol. Dis.* 54, 82–93. doi: 10.1016/j.nbd.2013.02.007

Ferreira, J., da Silva, G. L., and Calixto, J. B. (2004). Contribution of vanilloid receptors to the overt nociception induced by B_2 kinin receptor activation in mice. *Br. J. Pharmacol.* 141, 787–794. doi: 10.1038/sj.bjp.0705546

Hall, J. M. (1992). Bradykinin receptors: pharmacological properties and biological roles. *Pharmacol. Ther.* 56, 131–190. doi: 10.1016/0163-7258(92)90016-s

Hall, J. M. (1997). Bradykinin receptors. *Gen. Pharmacol.* 28, 1–6. doi: 10.1016/S0306-3623(96)00174-7

Hess, J. F., Borkowski, J. A., Stonesifer, G. Y., MacNeil, T., Strader, C. D., and Ransom, R. W. (1994). Cloning and pharmacological characterization of bradykinin receptors. *Braz. J. Med. Biol. Res.* 27, 1725–1731.

Julius, D., and Basbaum, A. I. (2001). Molecular mechanisms of nociception. *Nature* 413, 203–210. doi: 10.1038/35093019

Kawaguchi, A., Sato, M., Kimura, M., Ichinohe, T., Tazaki, M., and Shibukawa, Y. (2015). Expression and function of purinergic $P2Y_{12}$ receptors in rat trigeminal ganglion neurons. *Neurosci. Res.* doi: 10.1016/j.neures.2015.04.008 [Epub ahead of print].

Kitakoga, O., and Kuba, K. (1993). Bradykinin-induced ion currents in cultured rat trigeminal ganglion cells. *Neurosci. Res.* 16, 79–93. doi: 10.1016/0168-0102(93)90075-2

Kuroda, H., Sobhan, U., Sato, M., Tsumura, M., Ichinohe, T., Tazaki, M., et al. (2013). Sodium-calcium exchangers in rat trigeminal ganglion neurons. *Mol. Pain* 9:22. doi: 10.1186/1744-8069-9-22

Luiz, A. P., Schroeder, S. D., Chichorro, J. G., Calixto, J. B., Zampronio, A. R., and Rae, G. A. (2010). Kinin B_1 and B_2 receptors contribute to orofacial heat hyperalgesia induced by infraorbital nerve constriction injury in mice and rats. *Neuropeptides* 44, 87–92. doi: 10.1016/j.npep.2009.10.005

Ma, Q. P., Hill, R., and Sirinathsinghji, D. (2000). Basal expression of bradykinin B_1 receptor in peripheral sensory ganglia in the rat. *Neuroreport* 11, 4003–4005. doi: 10.1097/00001756-200012180-00020

Mantyh, P. W., Koltzenburg, M., Mendell, L. M., Tive, L., and Shelton, D. L. (2011). Antagonism of nerve growth factor-TrkA signaling and the relief of pain. *Anesthesiology* 115, 189–204. doi: 10.1097/ALN.0b013e31821b1ac5

Mistry, S., Paule, C. C., Varga, A., Photiou, A., Jenes, A., Avelino, A., et al. (2014). Prolonged exposure to bradykinin and prostaglandin E2 increases TRPV1 mRNA but does not alter TRPV1 and TRPV1b protein expression in cultured rat primary sensory neurons. *Neurosci. Lett.* 564, 89–93. doi: 10.1016/j.neulet.2014.02.006

More, A. S., Kim, H. M., Khang, G., Hildebrandt, T., Bernlöhr, C., Doods, H., et al. (2014). Des-Arg9-bradykinin causes kinin B_1 receptor mediated endothelium-independent contractions in endotoxin-treated porcine coronary arteries. *Pharmacol. Res.* 90, 18–24. doi: 10.1016/j.phrs.2014.09.001

Ochoa, J. L. (2009). Neuropathic pain: redefinition and a grading system for clinical and research purposes. *Neurology* 72, 1282–1283. doi: 10.1212/01.wnl.0000346325.50431.5f

Patwardhan, A. M., Berg, K. A., Akopain, A. N., Jeske, N. A., Gamper, N., Clarke, W. P., et al. (2005). Bradykinin-induced functional competence and trafficking of the δ-opioid receptor in trigeminal nociceptors. *J. Neurosci.* 25, 8825–8832. doi: 10.1523/jneurosci.0160-05.2005

Pesquero, J. B., Pesquero, J. L., Oliveira, S. M., Roscher, A. A., Metzger, R., Ganten, D., et al. (1996). Molecular cloning and functional characterization of a mouse bradykinin b1 receptor gene. *Biochem. Biophys. Res. Commun.* 220, 219–225. doi: 10.1006/bbrc.1996.0384

Regoli, D., Rizzi, A., Perron, S. I., and Gobeil, F. (2001). Classification of kinin receptors. *Biol. Chem.* 382, 31–35. doi: 10.1515/bc.2001.005

Rehn, M., Bader, S., Bell, A., and Diener, M. (2013). Distribution of voltage-dependent and intracellular Ca^{2+} channels in submucosal neurons from rat distal colon. *Cell Tissue Res.* 353, 355–366. doi: 10.1007/s00441-013-1643-5

Scholz, J., and Woolf, C. J. (2002). Can we conquer pain? *Nat. Neurosci.* 5(Suppl.), 1062–1067. doi: 10.1038/nn942

Simpson, P. B., Woollacott, A. J., Hill, R. G., and Seabrook, G. R. (2000). Functional characterization of bradykinin analogues on recombinant human bradykinin B_1 and B_2 receptors. *Eur. J. Pharmacol.* 392, 1–9. doi: 10.1016/s0014-2999(00)00046-7

Talbot, S., Théberge-Turmel, P., Liazoghli, D., Sénécal, J., Gaudreau, P., and Couture, R. (2009). Cellular localization of kinin B_1 receptor in the spinal cord of streptozotocin-diabetic rats with a fluorescent [Nα-Bodipy]-des-Arg9-bradykinin. *J. Neuroinflammation* 6:11. doi: 10.1186/1742-2094-6-11

Tiwari, M. M., Prather, P. L., and Mayeux, P. R. (2005). Mechanism of bradykinin-induced Ca^{2+} mobilization in murine proximal tubule epithelial cells. *J. Pharmacol. Exp. Ther.* 313, 798–805. doi: 10.1124/jpet.104.080408

Walker, K., Perkins, M., and Dray, A. (1995). Kinins and kinin receptors in the nervous system. *Neurochem. Int.* 26, 1–16; discussion 17–26. doi: 10.1016/0197-0186(94)00115-b

Wotherspoon, G., and Winter, J. (2000). Bradykinin B_1 receptor is constitutively expressed in the rat sensory nervous system. *Neurosci. Lett.* 294, 175–178. doi: 10.1016/s0304-3940(00)01561-5

Conflict of Interest Statement: The authors declare that the research was conducted in the absence of any commercial or financial relationships that could be construed as a potential conflict of interest.

全国の歯学部・歯科大学における歯科麻酔学卒前教育の実態調査

日本歯科麻酔学会卒前教育ワーキンググループ
谷口省吾　一戸達也　嶋田昌彦　城　茂治
椙山加綱　丹羽　均　宮脇卓也　吉田和市
小谷順一郎（前委員）

【要約】 日本歯科麻酔学会卒前教育ワーキンググループでは，全国の歯学部・歯科大学において学生に対する歯科麻酔学教育が十分に行われ，全身管理ができる歯科医師の養成に貢献していることを社会に伝えるという目的で，歯科麻酔学卒前教育に関する実態調査を行い検討した．

委員の所属する8大学でまずトライアルを行いブラッシュアップした後に，平成25年5月から8月にかけて全国の29大学の歯科麻酔学教育担当講座へアンケート調査を行った．アンケートは講義と実習に分けて行い，講義に関しては内容を12項目に分類し，時間数や実施学年などについて調査した．また，歯科麻酔学と関連の深い医科系科目の講義についても調査を行った．実習に関しては13項目に分類し時間数，実施学年，実習方法について調査を行った．

すべての大学で歯科麻酔学教育に必要な講義が行われていたが，大学により時間数において差が認められた．実施学年については4年生が多かった．実習に関しても必要な項目は実施していたが時間数や内容で大学間に差が認められた．実習形式は自験，相互実習，シミュレーション実習，見学実習，座学実習であった．講義と実習に関して時間数，項目，実習方法の基準を作成し，歯科麻酔学教育の標準化を図る，あるいはミニマムリクワイヤメントを作成する必要があると考えられた．

Key-words：QUESTIONNAIRE SURVEY, DENTAL ANESTHESIOLOGY, UNDERGRADUATE EDUCATION, DENTISTRY, DENTAL UNIVERSITY

Ⅰ．緒　言

臨床能力のある，社会から求められる歯科医師を養成するために，診療参加型臨床実習の開始，歯科医師臨床研修の必修化，共用試験の開始，モデル・コア・カリキュラムの改訂など，歯科医学教育はこの数年で大きく変化してきている．また，患者の高齢化や生活習慣病の増加など歯科医療を取り巻く社会情勢の変化により患者の状態評価や全身管理が重要視されるようになってきた．ガイドライン2000に始まる一次救命処置の普及，歯科外来環境体制加算制度の制定など医療安全も重視されるようになってきた．さらに，同意書を含むインフォームドコンセントなど患者中心の医療も謳われてきている．

このような歯科医学教育の変化に伴い，歯科麻酔学教育も少しずつ変化してきている．しかし，わが国の大学における歯科麻酔学に関する講義と実習が実際にどのような内容で，どれくらいの時間実施されているかは定かではない．歯科医学教育の実態に関しては全体の講義や実習時間に関しては調査がなされているが[1]，各診療科に関する報告は少ないのが現状である．歯科麻酔学においても卒前教育の実態は，平成13年に金子[2]らの「歯科医師の麻酔科研修のガイドライン策定に関する研究」のなかで一部調査されているのみで，調査内容も講義と実習の時間，およびそれぞれの全教科の時間数に占める割合が示されているのみである．

歯科麻酔学の卒前教育が全身管理のできる有能な歯科医師の養成に貢献していることを社会に周知するには，モデル・コア・カリキュラムに記載された目標を達成するために全国の歯学部・歯科大学において歯科麻酔学の講義と実習が十分に行われていることを示す必要がある．そのためには正確な調査により実態を把握して必要であれば歯科麻酔学の卒前教育における基準を作成すべきと考えられる．各大学で行われる講義や実習内容をできるだけ標準化することは，社会の信頼を得，歯科医学の安全性と質の向上，歯科医師の医療における地位の向上にも必要である．歯科医師の麻酔科研修や救急研修の妥当性にもつながる．日本歯科麻酔学会卒前教育ワーキンググループでは全国の歯学部・歯科大学における歯科麻酔学卒前教育の実態調査を行い，結果を分析した．

2015年3月15日受付

Ⅱ. 方　法

1. 調査方法

調査はアンケート形式で行った．アンケート内容については歯科麻酔学に関する講義と実習に分けて卒前教育ワーキンググループ委員の所属する大学でトライアルを行った後，再検討を行いアンケートを作成した．調査は平成25年5月から8月にかけて全国の29大学の歯科麻酔学卒前教育担当者に依頼し，平成24年度の実態について調査した．

2. 調査内容

講義に関しては，麻酔学総論，全身管理，局所麻酔，精神鎮静法，全身麻酔，日帰り全身麻酔，小児の麻酔管理，高齢者の麻酔管理，障害者の麻酔管理，歯科治療における全身的偶発症，心肺蘇生法，ペインクリニックに大きく項目を分類して，それぞれの項目について時間数や実施学年について調査した．また，歯科麻酔学と関係の深い医科系科目の講義について，時間数，講義科目および実施学年に関する調査を行った（Table 1）．

実習に関しては，歯科麻酔に関する医療面接，麻酔管理計画（対診書作成含む），バイタルサインの測定（モニタリング機器の取り扱いを含む），注射法，一次救命処置，二次救命処置（ICLS, ACLS），器具を用いた気道確保法，浸潤麻酔，伝達麻酔，モニタリングによる全身管理，笑気吸入鎮静法，静脈内鎮静法，全身麻酔法，その他に分類し，それぞれの項目について時間数や実習方法，担当診療科について調査を行った．また，実施学年についても調査した（Table 2）．大学名は特定しないこととし，さらにアンケートの質を高めるために回答責任者名とE-mail adressを記載してもらい，必要なら再確認できるようにした．

3. 解析

講義，実習の項目ごとに実施時間の平均値と標準偏差を算出するとともに実施時間ごとの大学数のヒストグラムを作成した．

Ⅲ. 結　果

すべての大学の歯科麻酔学講義・実習教育担当者から回答が得られた．

1. 講義（Fig. 1）

1）総講義時間

平均は44.3±11.6時間（23〜73時間）であった．

2）麻酔学総論

平均は94.0±52.1分（0〜270分）であった．行っていない大学もあったが，4年生以外に1年生の導入講義で行われていた．

3）全身管理

平均は527.8±211.0分（120〜1,200分）であった．

4）局所麻酔

平均は301.6±156.8分（90〜720分）であった．

5）精神鎮静法

平均は149.5±76.4分（60〜360分）であった．

6）全身麻酔

平均は586.7±272.4分（180〜1,395分）であった．

7）日帰り全身麻酔

平均は72.4±44.6分（0〜395分）であった．この項目の講義が行われていない大学もあったが，全身麻酔の項目で行われていた．

8）小児の麻酔管理

平均は61.2±33.5分（0〜150分）であった．この項目の講義が行われていない大学もあったが，いくつかの大学は小児歯科の講義などで行われていた．

9）高齢者の麻酔管理

平均は61.6±34.3分（0〜395分）であった．講義が行われていない大学もあったが，いくつかの大学は全身麻酔の項目で行われていた．

10）障害者の麻酔管理

平均は101.2±36.6分（0〜630分）であった．講義が行われていない大学もあったが，いくつかの大学は障害者歯科などで行われていた．

11）歯科治療における全身的偶発症

平均は152.8±109.0分（60〜600分）であった．

12）心肺蘇生法

平均は166.8±106.6分（60〜510分）であった．

13）ペインクリニック（顎顔面領域の神経性疾患）

平均は170.2±88.3分（45〜350分）であった．

14）医科系科目講義（Fig. 2）

平均は123.5±50.7時間（15〜196.5時間）と大学間で大きな差がみられた．科目は内科，外科，整形外科，耳鼻科，形成外科（または美容外科），眼科，小児科，脳外科，精神科（または心療内科），産婦人科，泌尿器科，皮膚科であった．内科はすべての大学で講義が行われていたが，それ以外では外科，皮膚科，耳鼻科，眼科，小児科，精神科（または心療内科）が多かった．また，内科以外はほとんど行っていない大学と10科目以上行っている大学とがあり，大きな差が認められた．

15）実施学年について

4年生で行っている大学が最も多かったが，3年生や5年生で行われている大学もあった．複数の学年で行って

Table 1 Questionnaire regarding lectures

1．麻酔学総論
(1) 麻酔の概念
(2) 麻酔と歯科麻酔の歴史
(3) 歯科麻酔の特徴
(4) その他
2．全身管理
(1) 麻酔学に必要な生理学
(2) 管理上問題となる全身疾患（医科疾患）
(3) 全身状態評価
(4) モニタリング
(5) 麻酔におけるインフォームドコンセント
(6) その他
3．局所麻酔
(1) 局所麻酔薬の作用機序
(2) 局所麻酔薬の種類と特徴
(3) 血管収縮薬
(4) 局所麻酔法
(5) 合併症とその対策
(6) その他
4．精神鎮静法
(1) 精神鎮静法の概念
(2) 吸入鎮静法
(3) 静脈内鎮静法
(4) その他
5．全身麻酔
(1) 全身麻酔の概念と方法
(2) 全身麻酔薬の作用機序
(3) 術前の全身状態評価
(4) 吸入麻酔薬
(5) 静脈麻酔薬
(6) 筋弛緩薬
(7) 麻薬
(8) 麻酔器と麻酔回路
(9) 術前管理
(10) 術中管理
(11) 術後管理
(12) 輸液と輸血
(13) 術中・術後麻酔合併症
(14) その他
6．日帰り全身麻酔（外来全身麻酔）
(1) 日帰り全身麻酔の特徴
(2) 適応と禁忌
(3) 日帰り全身麻酔の実際
(4) その他
7．小児の麻酔管理
(1) 小児の特徴
(2) 小児麻酔の実際
(3) 歯科小児麻酔の特徴
(4) その他
8．高齢者の麻酔管理
(1) 高齢者の生理的特徴
(2) 局所麻酔
(3) 精神鎮静法
(4) 全身麻酔法
(5) その他
9．障害者の麻酔管理
(1) 障害者の特徴と主な障害・疾患
(2) 術前管理
(3) 麻酔法の選択
(4) 術後管理
(5) その他
10．歯科治療における全身的偶発症
(1) 定義
(2) 全身的偶発症の種類と処置
(3) その他
11．心肺蘇生法
(1) 歴史
(2) 一次救命処置
(3) 二次救命処置
(4) その他
12．ペインクリニック
(1) 顎顔面痛患者の診断法
(2) 顎顔面領域の疼痛性疾患
(3) 顎顔面領域の麻痺性疾患
(4) その他

【医科系講義】
内科
外科
整形外科
耳鼻科
形成（美容）外科
眼科
小児科
脳外科
精神科（または心療内科）
産婦人科
泌尿器科
皮膚科

いる大学もあった．一部の大学で心肺蘇生法が3学年で行われていた．医科系科目は3年生から5年生で主に行われていた．

Table 2 Questionnaire regarding practical training

	時間数	実施学年	実習方法	担当診療科
1．歯科麻酔に関する医療面接				
2．麻酔管理計画（対診書作成含む）				
3．バイタルサインの測定（モニタリング機器の取り扱いを含む）				
4．注射法				
5．一次救命処置				
6．二次救命処置				
1）二次救命処置				
2）器具を用いた気道確保法				
7．浸潤麻酔				
8．伝達麻酔				
9．モニタリングによる全身管理				
10．精神鎮静法				
1）笑気吸入鎮静法				
2）静脈内鎮静法				
11．全身麻酔法				
12．その他				

2．実習

1．実習時間と実習方法（Fig. 3, Table 3）

1）総実習時間

実習時間の平均は36.6±24.6時間（12～120時間）であった．大学によって大きな差がみられた．

2）歯科麻酔に関する医療面接

実習時間の平均は68.1±86.4分（0～320分）であった．1校が320分と突出して多かった．実習を行っている大学は18校で見学実習が13校と最も多く，その他に座学実習，相互実習，シミュレーション実習などを行っていた．

3）麻酔管理計画（対診書作成含む）

実習時間の平均は106.2±163.8分（0～900分）であった．実習を行っていない大学が7校あった．15時間ほどかけている大学が1校あったが，実症例の計画立案と発表が行われていた．

4）バイタルサインの測定（モニタリング機器の取り扱いを含む）

実習時間の平均は159.7±98.8分（60～420分）で，すべての大学で行われていた．実習形式は学生相互実習が主体で4年生，5年生と2学年にわたり行っている大学が12校あった．3つの学年で行われている大学は2校であった．

5）注射法

実習時間の平均は93.4±84.5分（0～360分）であった．実施していない大学が7校あった．実習形式では相互実習（10校）とシミュレーション実習（9校）が多かった．実習内容として，筋肉注射，静脈路確保，アレルギー検査法などがあった．

6）一次救命処置

実習時間の平均は235.2±111.4分（60～510分）で，すべての大学で行われていた．実習形式はすべてシミュレーション実習で，4年生と5年生など2学年にわたり行っている大学が14校と最も多かった．3つの学年にわたって行っている大学が4校あった．

7）二次救命処置（ICLS, ACLS）

実習時間の平均は52.2±106.4分（0～540分）であった．実施していない大学が16校あった．実施していた13大学において6大学がシミュレーション実習，7大学が座学実習であった．シミュレーション実習ではマネキンとPCによるシミュレーターの使用やビデオ供覧が行われていた．

8）器具を用いた気道確保法

実習時間の平均は74.5±55.6分（0～180分）であった．実施していない大学が7校あった．方法としてはシミュレーション実習が行われていた．

9）浸潤麻酔

実習時間の平均は152.5±169.7分（30～900分）であった．相互実習が20校と最も多かった．シミュレーション実習を行った後，自験や相互実習を行っている大学もあった．自験は口腔外科や他科で抜歯などの歯科治療の実習の際に行われていた．

10）伝達麻酔

実習時間の平均は125.2±160.3分（0～900分）であっ

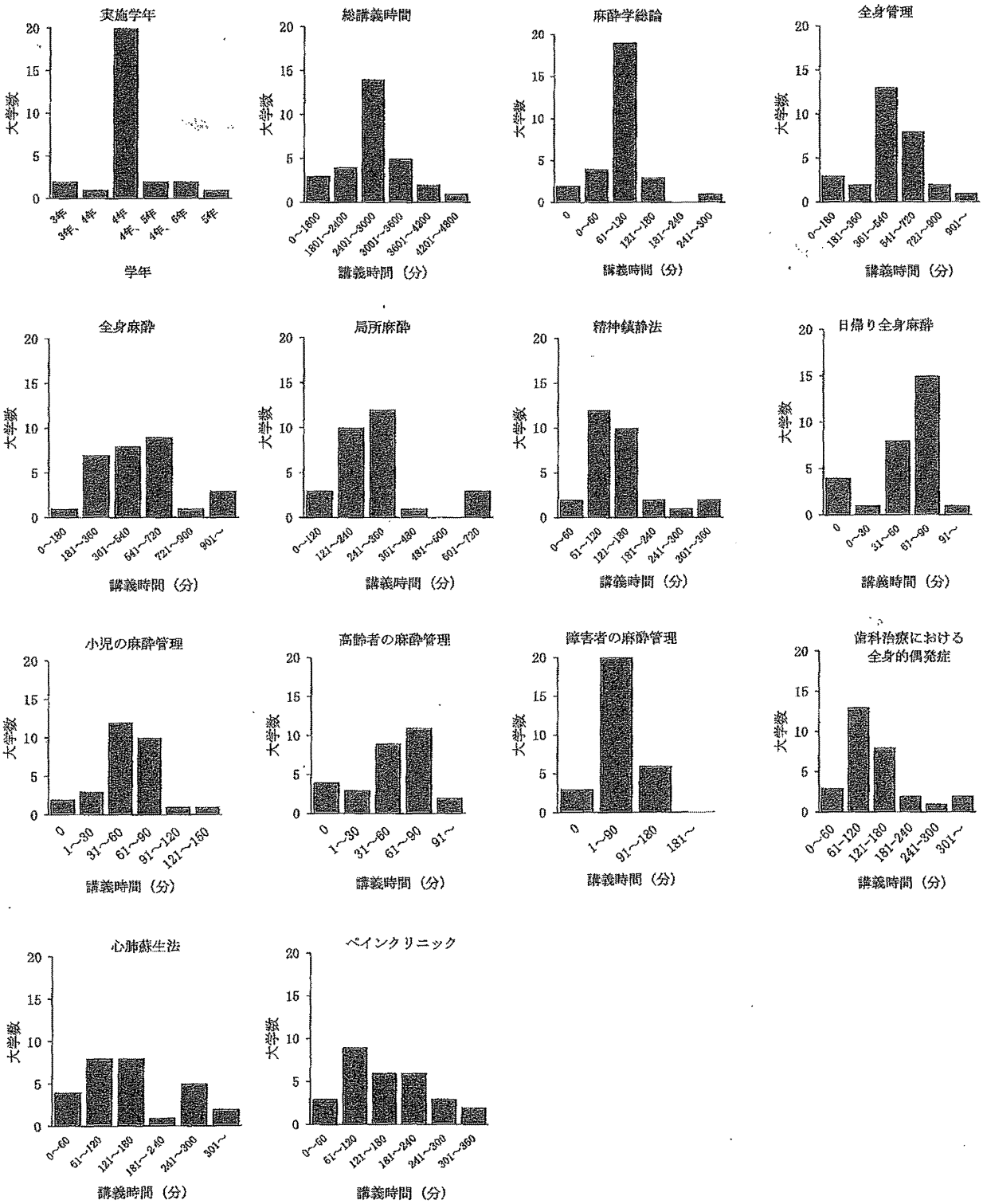

Fig. 1 Results of questionnaire regarding lectures

た．相互実習を行っている大学が14校と約半数を占めた．相互実習を行っていない大学ではシミュレーション実習や実際の症例見学が行われていた．シミュレーション実習を行った後，自験や相互実習を行っている大学もあった．自験は口腔外科や他科で抜歯などの歯科治療の実習の際に行われていた．

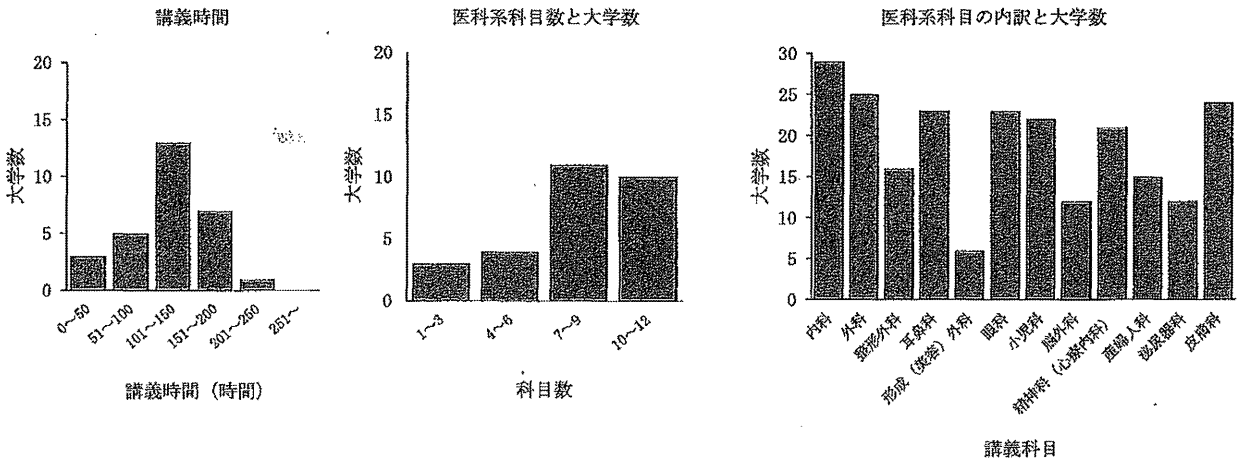

Fig. 2 Results of questionnaire regarding lectures on medical department

11) モニタリングによる全身管理

実習時間の平均は143.8±176.0分(0~630分)で，実施していない大学が10校あった．自験を行っている大学もあった．

12) 笑気吸入鎮静法

実習時間の平均は119.8±101.6分(0~540分)であった．学生相互実習を行っている大学が22校と多く，それ以外では見学実習が行われていた．

13) 静脈内鎮静法

実習時間の平均は253.6±488.1分（0~2,700分）であった．相互実習を行っている大学はなく，行っている大学では見学実習が多かった．

14) 全身麻酔法

実習時間の平均は494.5±517.0分（60~2,400分）で大学間に大きな差が認められた．ほとんどが見学実習であったが，1校のみ症例がないときにシミュレーション実習が行われていた．マスク換気と喉頭展開のみではあるが自験を行っていた大学もあった．

15) その他

ペインクリニック見学や救急薬品解説などが行われていた．

16) 実施学年について

主に4年生と5年生の複数の学年で行われていたが，4年生から5年生，5年生から6年生の2学年にわたって行っている大学もあった．バイタルサインの測定，一次救命処置は複数の学年で行っている大学が多く，なかには3つの学年で行っている大学もあった．

17) 実習担当診療科

実習担当科はほとんど歯科麻酔科であったが，歯科麻酔科以外では浸潤麻酔や伝達麻酔は口腔外科や他の診療科で歯科治療の実習の際に行われていた．

Ⅳ. 考　察

歯科麻酔学教育については，歯科医学教育に必要な最小限度の内容と範囲を体系的に明示し，教育上の基準を定めた歯科医学教授要綱[3]やその行動目標である歯学教育モデル・コア・カリキュラムなどに基づいて行われ，適宜改訂されている[1]．臨床研修の必修化，共用試験の開始により歯科医学教育だけでなく歯科麻酔学教育に関する環境は大きく変化してきている．共用試験は診療参加型実習の充実を図り，社会の求める優れた歯科医師を育成するために臨床実習開始前に行うもので，平成18年より開始されたが，大学による歯学教育に大きな影響を及ぼしている．臨床実習に関しては記憶主体の学習，見学型の臨床実習，基本的診療能力の不足，科目担当教員まかせの教育内容と学生評価などの問題点を解決し，一連の臨床の流れを一人の患者で経験できるような診療参加型実習を行うことが推奨されている．最近では文部科学省による「自験」の定義の再確認と臨床実習取り組み状況のフォローアップにより，より適切な臨床実習が行われるようになってきている[4]．

大学にとどまらず，社会においても歯科医学を取り巻く環境は大きく変化してきている．患者の高齢化や生活習慣病の増加など社会情勢の変化を受け，歯科医療における全身管理の重要性が認識されるようになってきた．さらに平成12年の一次救命処置ガイドラインの改訂(ガイドライン2000)以来，一次救命処置講習会に参加する歯科医師の増加や平成20年の歯科外来診療環境体制加算の制定[5]なども安全な歯科医療に貢献している．これらの流れを受け大学の歯学教育，特に歯科麻酔学教育においても医療安全や全身管理が重要視されるようになってきた．

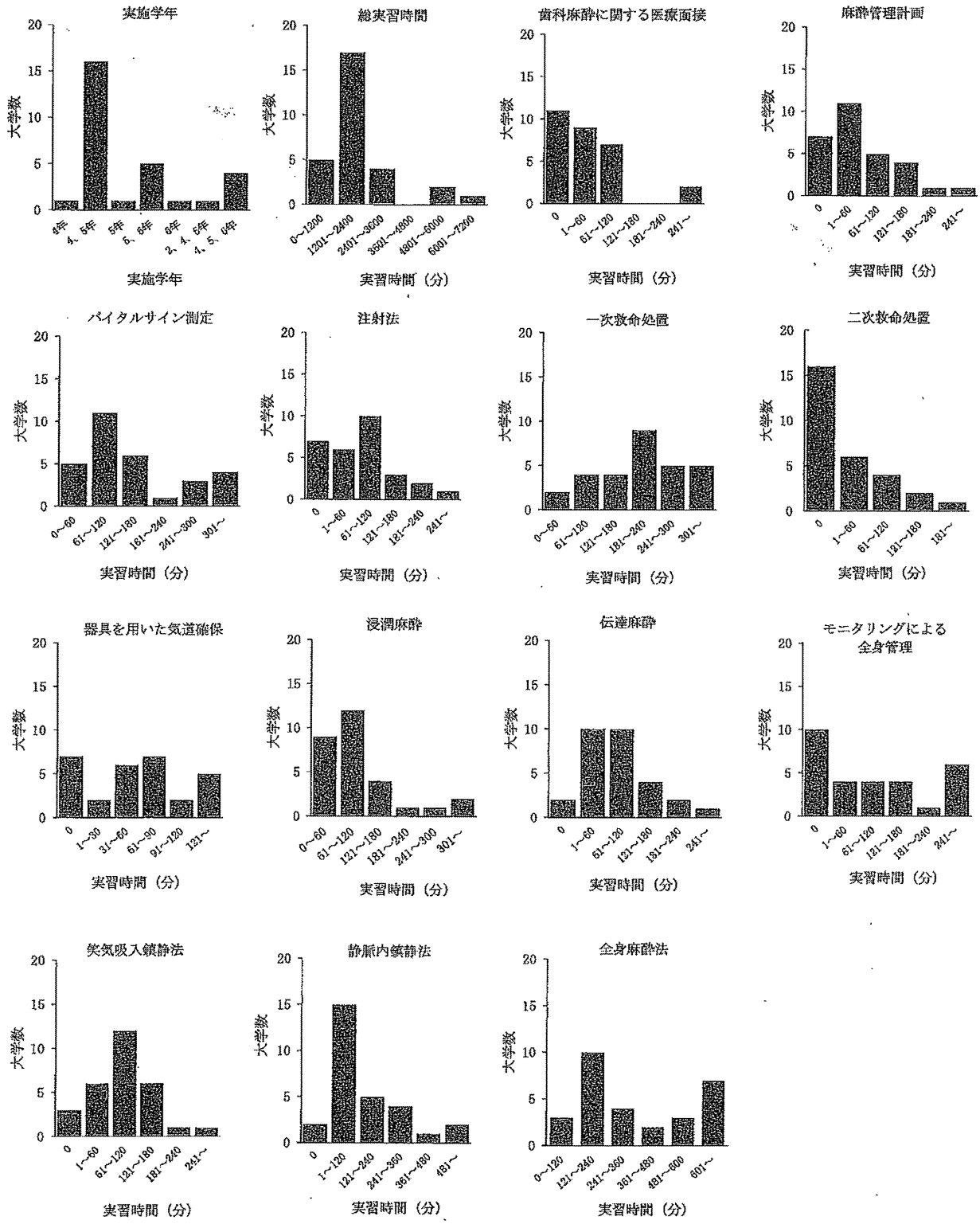

Fig. 3 Results of questionnaire regarding practical training